Larhyss Journal, ISSN 1112-3680, n°56, Dec 2023, pp. 77-106

PREDICTIVE MODELLING OF DAILY DRIED SLUDGE PRODUCTION IN FULL-SCALE WASTEWATER TREATMENT PLANT USING DIFFERENT MACHINE LEARNING COMBINED WITH EMPIRICAL MODE DECOMPOSITION

***ZAIDI K.* [1,2*], *DJEDDOU M.* [3], *SEKIOU F.* [1,3],**
***HAMEED I.A.* [4], *SHAWAQFAH M.* [5]**

[1] Department of Hydraulics, Faculty of Sciences and Applied Sciences, University of Oum el Bouaghi, Algeria
[2] Natural Resources Laboratory and Management of Sensitive Environments (RNAMS), University of Oum el Bouaghi, Algeria
[3] Research Laboratory in Subterranean and Surface Hydraulics (LARHYSS), University of Biskra, Algeria
[4] Department of ICT and Natural Sciences, Faculty of Information Technology and Electrical Engineering, Norwegian University of Science and Technology (NTNU), Postboks 1517, 6025 Ålesund, Norway
[5] Al Al-Bayt University, Engineering Faculty, Civil Engineering Department, Mafraq, 25113, Jordan

(*) *kaddour.zaidi@univ-oeb.dz*

Research Article – Available at http://larhyss.net/ojs/index.php/larhyss/index
Received July 16, 2023, Received in revised form November 15, 2023, Accepted November 18, 2023

ABSTRACT

Sewage sludge has gained importance and become a general significant environmental concern due to the presence of dangerous heavy metals and organic pollutants. In this study, various simple machine learning (ML) models, namely, multilayer perceptron neural network (MLPNN), radial basis function neural network (RBFNN), generalized regression neural network (GRNN), extreme learning machine (ELM), and support vector regression (SVR), were compared with hybrid empirical mode decomposition (EMD-ML) and variational mode decomposition (VMD-ML). The RBFNN model had the best results for the simple ML models because of the best performance parameters compared with other simple models. The EMD-ML models' results revealed that the EMD-MLPNN model had high performance parameters and lower errors compared with the remaining models, and the VMD-ML models' findings indicated that the VMD-GRNN model had good statistical indicator parameters compared to other models. The qualitative comparison findings indicated that the EMD-MLPNN method produced the best predictive performance for the training phase with R = 0.9729 and MAE = 2.5521 and during the testing phase with R = 0.9909 and MAE = 2.1144 in comparison to the VMD-GRNN and the RBFNN. The combination of EMD-ML improved ML accuracy, especially for EMD-MLPNN, in predicting daily dried sludge production in WWTPs.

Keywords: Predictive Modeling, Daily Dried Sludge Production, Wastewater Treatment Plant, Machine Learning, Empirical Mode Decomposition, Variational Mode Decomposition.

INTRODUCTION

Sludge production is intertwined with the wastewater treatment process (Gaouar and Gaouar, 2016; Aroua-Berkat and Aroua, 2022). Any augmentation in wastewater treatment can lead to massive quantities of sewage sludge (Hbaiz et al., 2014; El Ghammat et al., 2019). Because of the putrefaction of the organic composites of sewage sludge and the struggle to dispose of it, the progressive accumulation of large amounts of sewage sludge from different sources, whether home and industrial wastewaters, has a negative impact on the environment (Pai et al., 2011). It is mostly used to fertilize agriculture as a better option compared to incineration and landfilling, which has been acknowledged globally as a potential technique to manage this source since it may reduce pollution and add to the circular economy. If utilized as an organic fertilizer, the sludge organic matter content can refine soil physical, chemical, and biological qualities and induce beneficial plant yield responses. The fundamental restriction is the safety of sewage sludge reuse. Because of possibly concentrated toxic substances such as heavy metals, microorganisms, and emerging contaminants, sludge reuse may pose a concern. This study aims to help managers and operators of waste water treatment plants (WWTPs) predict the daily quantities of sewage sludge and show how to utilize the spaces designated for drying. Therefore, through the best model obtained from the results of this study, the daily amount of sludge can be predicted, and the problem of sludge accumulation and spread over days and weeks can be managed to reduce environmental risks and improve treatment efficiency.

During the last decade, the application of artificial intelligence (AI) techniques has received growing interest from researchers, especially in the field of engineering. Among the techniques used, artificial neural networks (ANNs) and support vector machines (SVMs) have shown very good results in the prediction task (Wang et al., 2015; Heddam and Kisi, 2017; Khatri et al., 2019; Leong et al., 2019; Najafzadeh and Zeinolabedini, 2019; Djeddou et al., 2020; Hong et al., 2020; Cai et al., 2021; Djeddou et al., 2021a; Djeddou et al., 2021b; Djeddou et al., 2021c; Rayi et al., 2022; Yang et al., 2022; Zerouali et al., 2023).

There has been a dominant innovation in time-frequency hybrid models, frequently employed in hydrology and hydraulic engineering, to analyze time sequences. Abda and Chettih (2018) used ANN, adaptive neuro-fuzzy inference system (ANFIS) coupled with wavelet transform (WT) and empirical mode decomposition (EMD) models to forecast daily flows of the Sebaou River, Algeria. The findings showed that the hybrid models

WT-ANFIS and EMD-ANFIS performed substantially better than the other models. Fouchal and Souag-Gamane (2019) evaluated ANN and WT-ANN hybrid model accuracy to forecast monthly flow in northern Algeria's humid and semiarid regions. The findings indicated that the second model performed better than the first model. Li et al. (2019) employed ANN, WT-ANN, EMD-ANN, and ensemble empirical mode decomposition (EEMD) combined with ANN for forecasting long-term daily stream flow. EEMD-ANN was shown to be the best model. Zakhrouf et al. (2020) used a feed forward back propagation neural network (FFBPNN), ANFIS, and WT-FFBPNN to forecast the stream flow in the Seybous River, Algeria, and WT-FFBPNN was the best model among the remaining models. Using ANN, ANFIS, WT-ANN, and WT-ANFIS models, Abda et al. (2021) sought to forecast the daily flows of the Sebaou River. It was proven that the hybrid model WT-ANFIS was the best compared to the remaining models. Song et al. (2021), trying to predict water quality parameters in two rivers in China, used a multilayer perceptron neural network (MLPNN), support vector regression (SVR), least square support vector machine (LSSVM), sparrow search algorithm (SSA) combined with LSSVM, variational mode decomposition (VMD) combined with LSSVM, and VMD-SSA-LSSVM. The findings showed that the VMD-SSA-LSSVM model proved its efficacy and superiority compared to the remaining models. Ahmed et al. (2022) used six machine learning (ML) and five decomposition models to forecast the dissolved oxygen (DO) of the Surma River, Bangladesh, and they indicated that maximum overlap discrete wavelet transformation combined with multivariate adaptive regression spline (MODWT-MARS) was the best model. Yelmiz (2022) utilized ANN, discrete wavelet transform (DWT) and additive wavelet transform (AWT) coupled with ANN to predict stream flow, and the results indicated the usefulness of AWT–ANN, as it was proven to be the best when compared to the other models.

For simple and hybrid models, AI methods were used as modeling tools to address environmental engineering problems, especially to assess WWTP performance. Belanche et al. (1999) concluded that the performance of a fuzzy heterogeneous neural network (FHNN) to predict biochemical oxygen demand (BOD), chemical oxygen demand (COD), and total suspended solid (TSS) in Catalonia WWTP surpassed other samples of ANNs. Gontarski et al. (2000), aiming to predict the removal of total organic carbon (TOC) in Rhodiaco Ltda. WWTP, employed the FFBPNN model. ANNs were used by Onkal-Engin et al. (2005) to show a fair link between sewage odor and WWTP BOD. Mjalli et al. (2007) used an ANN model that performed well in modeling the amount of BOD, COD, and TSS of the effluent and returned sludge in the Doha WWTP. Nasr et al. (2012) also confirmed that the FFBPNN model can be used as a tool to estimate the efficiency of the Alexandria WWTP. Boniecki et al. (2012) used ANN to predict ammonia emissions from sewage sludge composting. Verma et al. (2013) employed various AI models to predict TSS and determined that the FFBPNN model was the finest option in the Demoines WWTP. The concentrations of the water quality metrics COD and BOD for WWTPs were evaluated in Zare Abyaneh's study (2014), and the findings showed that the ANN model outperformed the multivariate linear regression (MLR) model. Djeddou and Achour (2015) examined the use of the ANN technique for the prediction of the sludge volume index (SVI) municipal in Batna WWTP. Guo et al. (2015), at the Ulsan WWTP, discovered that the SVM model outperformed the ANN technique when predicting total nitrogen concentration. Huang and Chen (2015) utilized FFBPNN and a generalized regression neural network (GRNN) to predict the thin layer design in municipal sewage sludge and concluded that FFBPNN was the best model. Recently, another study proved that a recurrent neural network (RNN) with explainable AI can predict SVI and interpret the prediction result in the Wisconsin WWTP (Wongburi and Park, 2022).

Hanbay et al. (2008) observed that hybrid WT-ANN was effective when gathering TSS sets of data in assessing Malatya WWTP performance in Turkey. Bagheri et al. (2015) stated that the ameliorated AI techniques' performance showed that feed forward neural network combined with genetic algorithm (FFNN-GA) method gave correct estimation for SVI parameter than that found through radial basis function neural network (RBFNN) combined with GA model in Ekbatan WWTP, Tehran. Baki and Aras (2018) predicted the BOD at a shorter time with a lower cost using three methods: multilayered (ML), teaching learning-based optimization (TLBO), and artificial bee colony (ABC) coupled with ANN in the Hurma WWTP, Turkey. Their results showed that ML-ANN is the best method compared to the other two methods. In the study of Cong and Yu (2018), it was proven that hybrid WT-ANN brought about better concise prediction of water quality indications for WWTP than ANN and SVM approaches. Najafzadeh and Zeinolabedini (2018) employed simple models: gene expression programming (GEP), model tree (MT), and evolutionary polynomial regression (EPR) combined with WT to predict sewage sludge quantity. WT-MT proved to be the best model in the Kerman WWTP. Zeinolabedini and Najafzadeh (2019) compared the performance of the FFBPNN, RBFNN, WT-FFBPNN, and WT-RBFNN models in sewage sludge quantity prediction, and the third model was indicated to be the most superior. Recently, another study utilized FFBPNN and principal component analysis (PCA) combined with FFBPNN to predict digested sludge in the Aïn Beïda WWTP (Djeddou et al., 2021a). The results proved that the hybrid PCA-FFBPNN was superior to the other model.

The current study was carried out using four parameters as input variables and daily dried sludge production (DDSP) as the output in the Aïn Beïda WWTP, Algeria. DDSP was predicted using machine learning (ML) models involving a multilayer perceptron neural network (MLPNN), radial basis function neural network (RBFNN), generalized regression neural network (GRNN), extreme learning machine (ELM), and support vector regression (SVR). A comparative study of simple and hybrid ML mode performance was conducted to find the best model in the prediction task.

This paper is organized as follows. The materials, methods, and data utilized for the current study are detailed in Section 2. Section 3 elaborates on the results and discusses them in detail. Finally, in the conclusion, a summary of the main findings that need to be regarded to benefit future research in the field of WWT engineering is provided in Section 4.

MATERIALS AND METHODS

Case Study

Aïn Beïda is a city situated in northeastern Algeria, Oum El Bouaghi. With respect to the geographical proprieties, the province has an altitude of minimal 940 m and a maximal 1.120 m above sea level, a latitude that equals 35°47'47" N, and a longitude of 7°23'24" E. It has a population of approximately 118 433 people, which makes it the largest city in the Wilaya, and has an area of 58.88 km2. Its WWTP started working in 2014 and was mapped out for a population of approximately 140 000. The location of this plant is far 3 km northeast of Aïn Beïda, with geographical location details of 35°47'22.24" N, 7°20'27.18" E at an altitude of 930 m. The plant's schematic portrayal is illustrated in Fig. 1. The area of such a plant is 180 ha, and its design capacity is 16840 m3/day. More technical information is displayed in Table 1. The Aïn Beïda WWTP process is schematically presented in Fig. 2.

Table 1: Technical information of the Aïn Beïda WWTP

Parameters	2015 kg.day^{-1}		Horizon 2033 m^3.day^{-1}
COD daily load	14 263	Maximum daily flow	1 736
BOD_5 daily load	7 560	Mean flow in dry time	25 260
TSS daily load	9 800	Peak flow in rainy weather	4 340
Nominal load (equivalent person)	210 000	Total phosphorus content	15

Figure 1: Aïn Beïda WWTP location (Google, 2023)

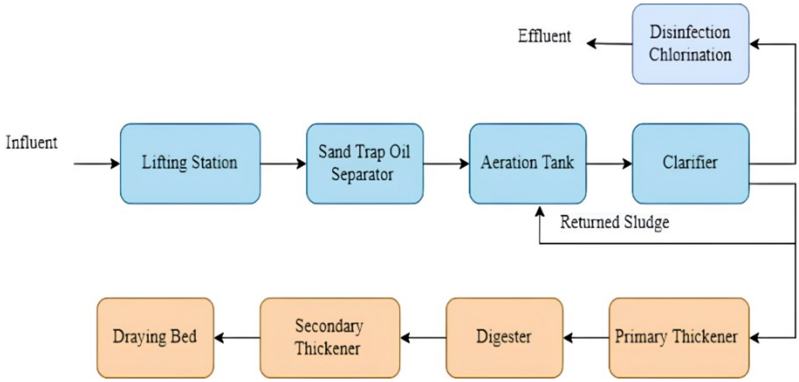

Figure 2: Process scheme of the Aïn Beïda WWTP

Data Description

In this investigation, datasets of the Aïn Beïda WWTP from 2014 to 2022 were used to constitute the models suggested. Table 2 displays the dataset statistical parameters used to establish the models. Fig. 3 shows the DDSP data. Specifically, datasets (given by a programmable robot named IHM SCADA and provided by the manager of the Aïn Beïda WWTP) were gathered by the researchers in four and a half years starting in January 2018. Such data (2638) were taken from the daily values of the WWTP. They have five parameters: influent rate flow, effluent rate flow, excessed sludge, and thickened sludge that served as the inputs; dried sludge was analyzed as an output. Fig. 4 illustrates the correlation matrices between the input and output variables. The datasets were normalized and randomly subdivided into two parts for training and testing phases. Eighty percent of the datasets were considered for the training phase. The remaining 20% were devoted to testing (Baki et al., 2019; Djeddou et al. 2021a; Mansour-Bahmani et al., 2021).

Table 2: Statistical properties of inputs and output

Parameters (m^3/d)	**Min.**	**Max.**	**Mean**	**S.D.**	**C. v.**
			Training		
Influent rate flow	199.32	22893.13	9087.84	3109.94	0.34
Effluent rate flow	16.07	21560.34	7246.21	3063.09	0.42
Excessed Sludge	0	2089.77	638.5	275.59	0.43
Thickened Sludge	5.48	924.84	278.02	137.61	0.49
Dried Sludge	4.47	202.82	66.98	26.7	0.4
Parameters (m^3/d)	**Min.**	**Max.**	**Mean**	**S.D.**	**C. v.**
			Testing		
Influent rate flow	412.22	19759.17	10495.29	3443.33	0.33
Effluent rate flow	60.49	16721.56	9055.07	2982.07	0.33
Excessed Sludge	15.77	1709.35	858.14	298.72	0.35
Thickened Sludge	19.97	905.54	374.39	140.91	0.38
Dried Sludge	10.31	204.58	84.3	30.41	0.36

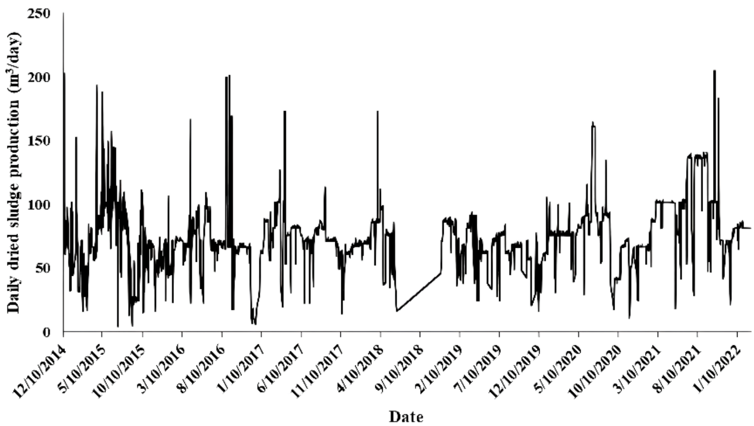

Figure 3: Daily dried sludge production data from 2014 to 2022

	Influent rate flow	Effluent rate flow	Excessed Sludge	Thickened Sludge	Dried Sludge
Influent rate flow	1				
Effluent rate flow	0.90328	1			
Excessed Sludge	0.32774	0.27306238	1		
Thickened Sludge	0.2813	0.2469044	0.917274	1	
Dried Sludge	0.30824	0.29010713	0.762381	0.756469	1

Figure 4: Pearson correlation matrices of the dataset

Modeling Approaches

Multilayer Perceptron Neural Network

The multilayer perceptron model is the most common machine learning model based on the back propagation (BP) learning technique for feed-forward neural networks (FFNNs). Inputs are multiplied by arbitrary weights (w_i) and summed by arbitrary bias (b) in a form of hypothesis ($Y = \sum_{i=1}^{n} X_i + b$). The hypothesis is then nonlinearized by hyperbolic tangent (*tansig*) as the activation function. A linear function (*purelin*) was used as the transfer function in the output layer. A schematic representation of the MLPNN architecture is shown in Fig. 5. MLP is a universal approximator (Haykin, 2009). The best number of perceptrons, number of hidden layers, and activation function were obtained using trial and error.

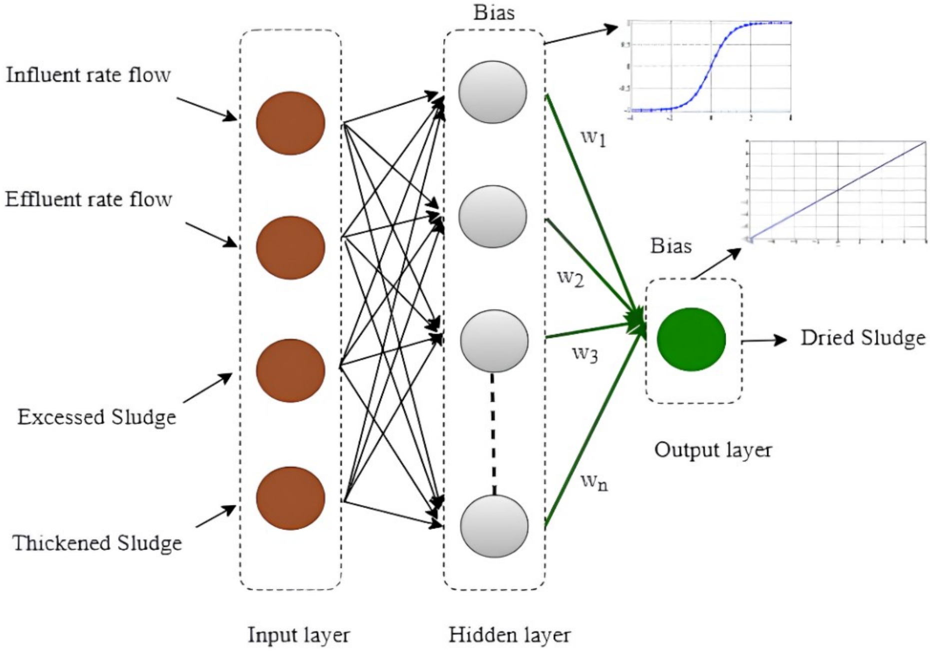

Figure 5: Schematic representation of the MLPNN model for predictive modeling of DS

Radial Basis Function Neural Network

Radial basis function neural networks (RBFNNs) are frequently employed in numerous engineering areas for predictive modeling. The RBFNN is depicted as a three-layer design, as shown in Fig. 6. Inputs are received by the first layer. The intermediate layer, which comprises a nonlinear RBF activation function, is the second layer. The prediction is made by the third layer (Moody and Darken, 1989; Haykin, 2009). The following is the equation for the RBFNN output:

$$y = \sum_{k=1}^{m} \omega_{jk}\theta_k(X) \quad (1)$$

where m is the number of basis functions; X is the input data vector; ω_{jk} is the weight of the connection between the basis function and output layer; and θ_k is the nonlinear function of unit j, which is typically a Gaussian of the form.

$$\theta_k(X) = exp\left(-\frac{\|X-\mu_k\|^2}{2\sigma_k^2}\right) \quad (2)$$

where X and μ are the input and center of the RBF unit, respectively, and σ_k is the spread of the Gaussian basis function.

The weights linking the hidden neurons to the outputs, centers, and width are regarded as critical keys in the construction and training of the RBFNN.

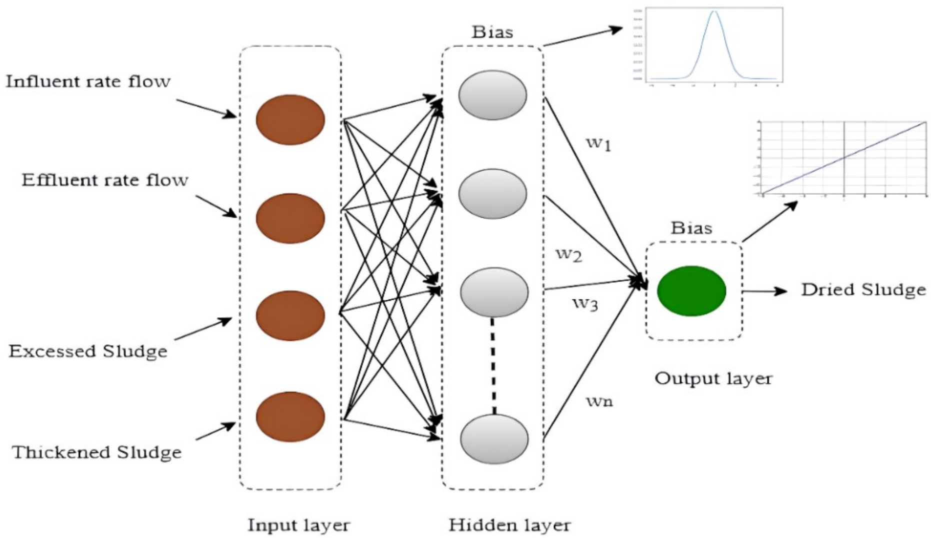

Figure 6: Schematic representation of the RBFNN model for predictive modeling of DS

Generalized Regression Neural Network

A generalized regression neural network (GRNN) is a kind of RBNN that is based on kernel regression and is a high-coherence network that can achieve near-zero prediction error for a large training set with simple function constraints. Its advantages are related to constancy. Fig. 7 depicts the GRNN architecture. Similar to the back-propagation network, it does not require an iterative learning process.

The problem of local minima does not occur in GRNN simulations (Specht, 1991). A specifically designed hidden neuron layer contains the input vector. The weights between the output layer and the newly formed hidden layer are given the desired value. The primary difference between the two neural networks (GR and RBF) is in how the values (w_{ij}) are computed.

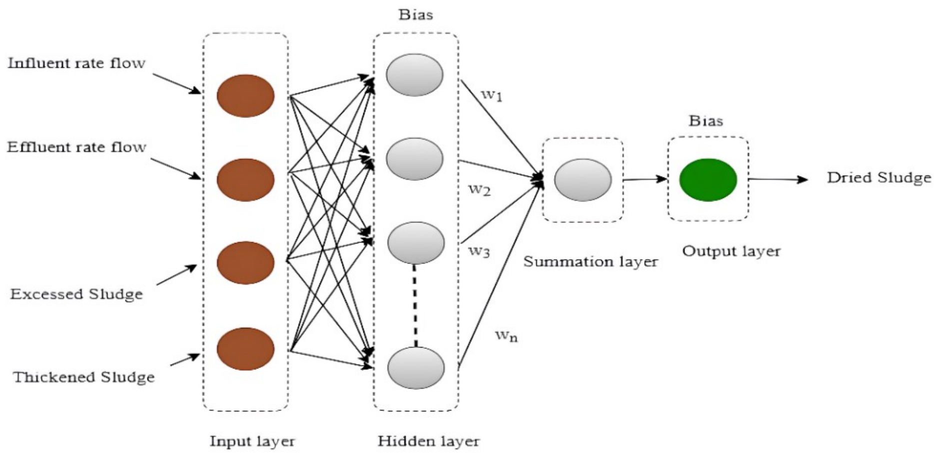

Figure 7: Schematic representation of the GRNN model for predictive modeling of DS

Extreme Learning Machine

Back propagation (BP), for example, uses specific criteria to alter the weights based on the batch in the training ensemble while training a single-layer feeder network (SLFN). The schematic of the extreme learning machine (ELM) is shown in Fig. 8. The weights in the ELM are determined at random. The underlying theory and method of the ELM are provided (Huang et al. 2006). SLFNs with random input weights may learn diverse training instances accurately with minimum error (Huang, 2003). The SLFN may be handled as a linear system by selecting the input weights and hidden layer biases. A generic inverse procedure for the hidden layer output matrices is used to calculate the output weights analytically. This method permits the ELM to outperform the feed-forward algorithm (Huang, 2003).

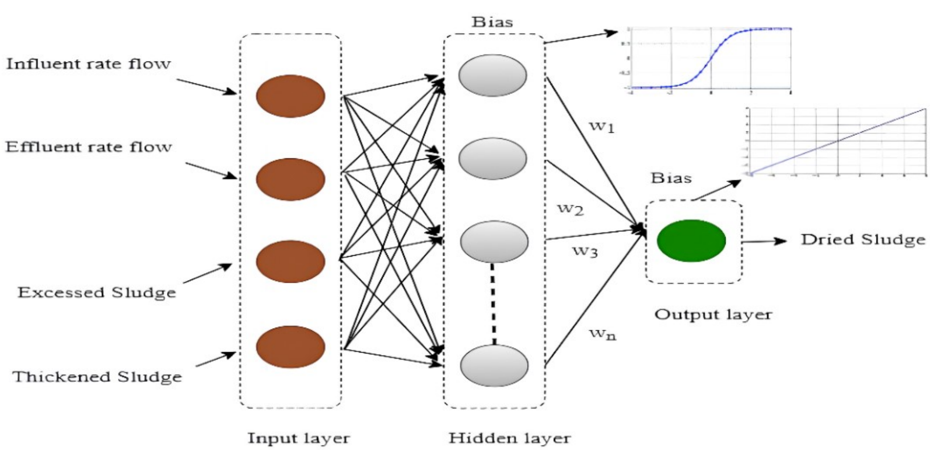

Figure 8: Schematic representation of ELM model for predictive modeling of DS

Support Vector Regression

Support vector regression (SVR) is a widely used modeling method in nonlinear modeling systems. The function fitting through SVR aims to decrease the error. The training points are the support vectors that are the nearest to the support vector machine main concept. There are decision functions that are accountable. The range from the nearest positive sample to a hyperplane and the range between the nearest negative and the hyperplane are shown (Vapnik, 1999). The schematic representation of SVR is shown in Fig. 9. This function can be formed as:

$$g(x) = w^T x + b \tag{3}$$

where *w* and *b* refer to the weight vector and intercept of the model to indicate in the optimal regression.

By minimizing the regularized risk function R(C), the coefficients *w* and *b* are estimated:

$$\textit{Minimize: } R(C) = C\sum_{i=1}^{N}(\xi_i - \xi_i^*) + \frac{1}{2}\|w\|^2 \tag{4}$$

$$\textit{Subject to: } \begin{cases} g_i - w^T x_i - b_i \leq \varepsilon + \xi_i, i = 1, \dots, N \\ w^T x_i + b_i - y_i \leq \varepsilon + \xi_i^*, i = 1, \dots, N \\ \xi_t, \xi_t^* \geq 0, i = 1, \dots, N \end{cases} \tag{5}$$

$\frac{1}{2}\|w\|^2$: weights vector norm; g_i: the desired value; and C: regularized constant determining the trade-off between the empirical error and the regularized term.

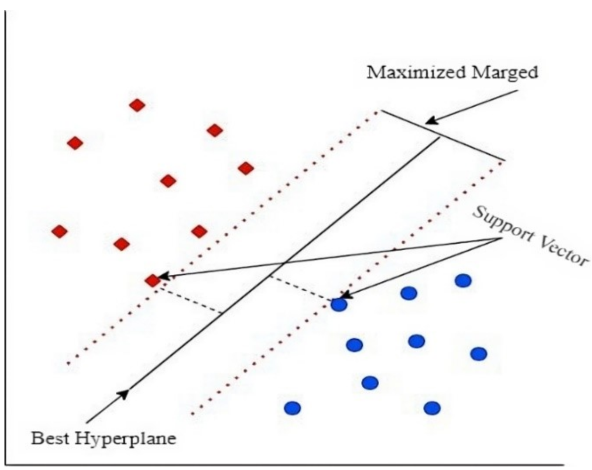

Figure 9: Schematic representation of the SVR model

Empirical Mode Decomposition

Huang et al. (1998) proposed the empirical mode decomposition (EMD) method to study nonlinear and nonstationary time series properties, which is also known as the Hilbert-Huang transformation (HHT). The model decomposes the original signal and the time signal analyzed into several intrinsic mode functions (IMFs) and a residual. Two requirements must be met by every IMF. The first requirement is that the total number of extremes in a time series has to match the total number of zero crossings or deviate by no more than one. The second is that the average of the higher and lower values must always be zero. A flowchart of the EMD process is displayed in Fig. 10. A time series $x(t)$ decomposed using the EMD technique can be written as the equation below based on the aforementioned criteria:

$$x(t) = r_n(t) + \sum_{i=1}^{n} c_i(t) \tag{6}$$

where $x(t)$ is the original signal, *n* is the number of IMFs, $c_i(t)$ is the *i-th* IMF component, and $r_n(t)$ is the residual component.

In the process of EMD, the initial step involves identifying the highest and lowest points of the time series. Subsequently, cubic spline interpolation is employed to create upper and lower envelopes by incorporating all the local maximum and minimum values, respectively. It has been demonstrated that the selection of extreme points is influenced by unusual data points in the original dataset, thereby impacting the determination of the envelopes. As a result, the resulting envelopes can contain a combination of both genuine signal information and abnormal points, leading to the occurrence of a phenomenon known as mode mixing.

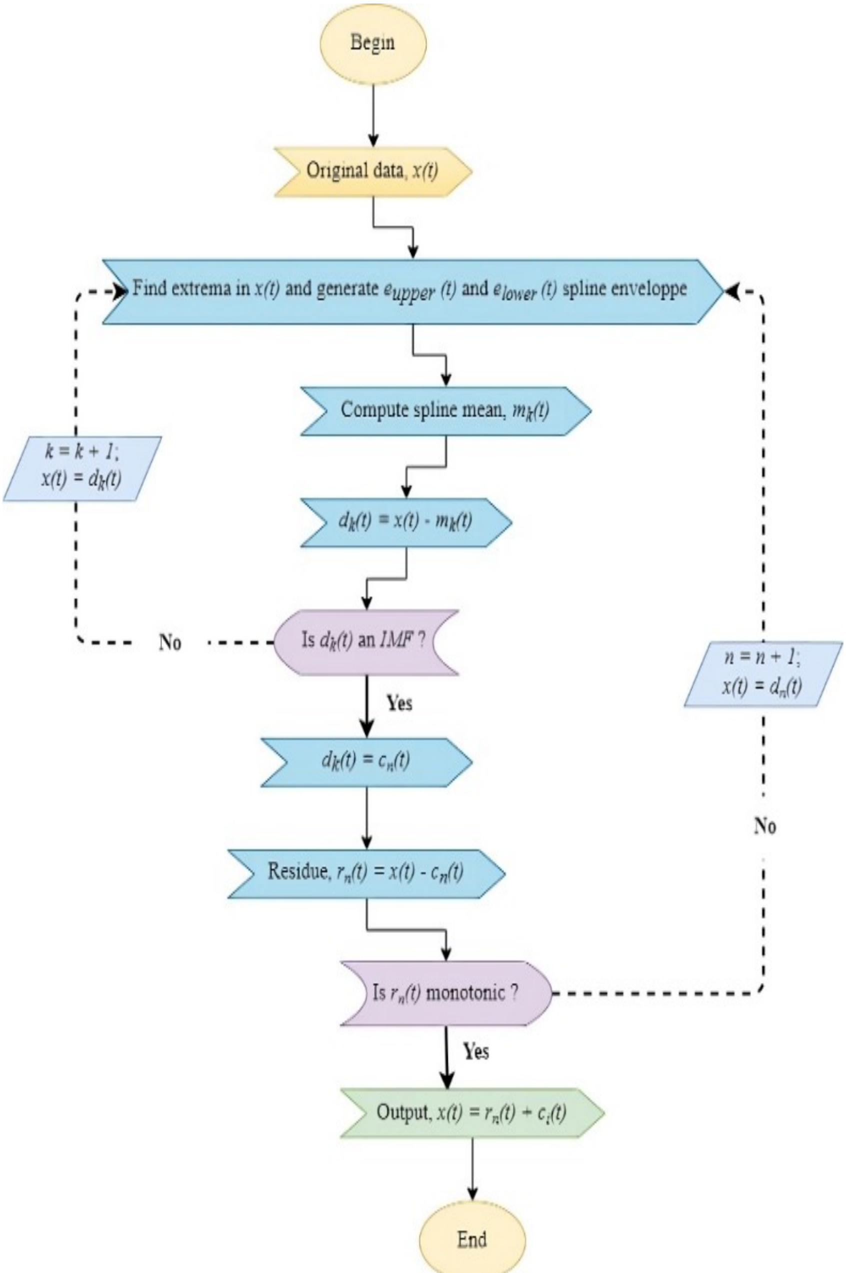

Figure 10: Flowchart of the EMD method

Variational mode decomposition

The variational mode decomposition (VMD) method is a recent adaptive and quasiorthogonal signal decomposition approach. A signal *x(t)* can be divided into *K* discrete subsignals or modes by the VMD method, and each component is regarded as compact around its own center frequency w_k. According to Dragomiretskiy and Zosso (2013), VMD is used to solve a restricted optimization issue. The flowchart of this model is shown in Fig. 11.

$$\min_{\{u_k\},\{\omega_k\}} = \left\{\sum_k \left\| \partial_t \left[\left(\delta(t) + \frac{j}{\pi t}\right) * u_k(t)\right] e^{-j\omega_k t} \right\|_2^2 \right\} s.t. \sum_k u_k = f \quad (7)$$

where $\{u_k\}$ is the k IMF obtained by decomposition and $\{\omega_k\}$ is the central frequency of the modal components. K is the total number of modal functions, $\delta(t)$ is the Dirac distribution, * denotes convolution, $e^{-j\omega_k t}$ is the center frequency of the modal function on the complex plane, with k as the center frequency of the modal function, $\sum_k$ is the number of decomposed components, and f is the observed signal.

The quadratic penalty term α and Lagrangian multipliers λ are introduced to transform the previous optimization problem into an unconstrained one Dragomiretskiy and Zosso (2013):

$$L(\{u_k\},\{\omega_k\},\lambda) = \alpha \sum_k \left\| \partial_t \left[\left(\delta(t) + \frac{j}{\pi t}\right) * u_k(t)\right] e^{-j\omega_k t} \right\|_2^2 + \|f(t) - \sum_k u_k(t)\|_2^2 + \langle \lambda(t), f(t) - \sum_k u_k(t) \rangle \quad (8)$$

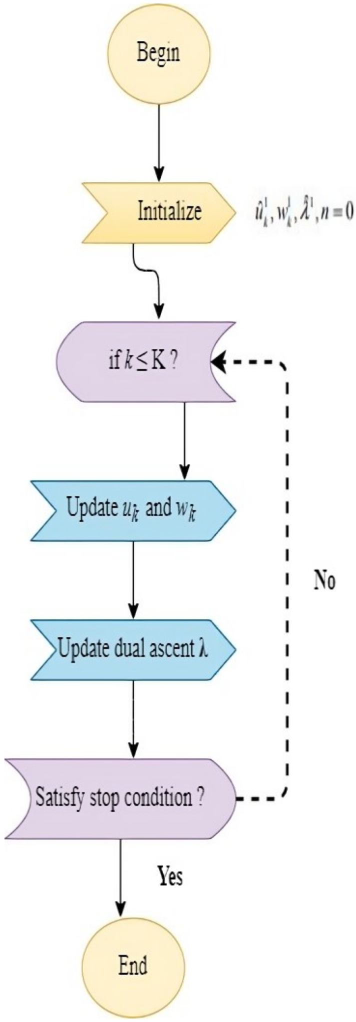

Figure 11: Flowchart of the VMD method

Performance Indicators

To assess the prediction ability of various ML, EMD-ML, and VMD-ML models, the correlation coefficient (R), the Nash-Sutcliffe efficiency coefficient (NSE), the root mean square error (RMSE), and the mean absolute error (MAE) for the training and testing phases are reported as follows:

$$R = \frac{\sum_{i=1}^{n}(DS_{o,i}-\overline{DS}_o)\times(DS_{p,i}-\overline{DS}_p)}{\sqrt{\sum_{i=1}^{n}(DS_{o,i}-\overline{DS}_o)^2 x \sum_{i=1}^{n}(DS_{p,i}-\overline{DS}_p)^2}} \tag{9}$$

$$NSE = 1 - \frac{\sum_{i=1}^{n}(DS_{p,i}-DS_{o,i})^2}{\sum_{i=1}^{n}(DS_{o,i}-\overline{DS}_o)^2} \tag{10}$$

$$RMSE = \sqrt{\frac{\sum_{i=1}^{n}(DS_{p,i}-DS_{o,i})^2}{n}} \tag{11}$$

$$MAE = \frac{1}{n}\sum_{i=1}^{n}\left|DS_{p,i} - DS_{o,i}\right| \tag{12}$$

where *n* is the number of observations; $DS_{o,i}$ is the observed value; $DS_{p,i}$ is the predicted value; and $\overline{DS}_o$ and $\overline{DS}_p$ are the averages of the observed and predicted values, respectively.

RESULTS AND DISCUSSION

The main goal of this research is to explore the capabilities of simple ML and hybrid ML for the predictive modeling of DDSP in the Aïn Beïda WWTP. All the results of this study were carried out using a PC equipped with an ASUS TUF FX505DT, AMD Rayzen ^{TM} 5 R5-3550H CPU at 3.7 GHz and 16 GB of RAM. All predictions were compared to choose the best model. The appropriate data for this study were chosen. In the EMD and VMD techniques, IMFs and residuals were found, followed by the stage normalization of datasets for all techniques (five ML, EMD, and VMD). Inputs and targets for different techniques were entered. The prediction for each technique was compared to choose the best one. The main steps of the study are schematically illustrated in Fig. 12.

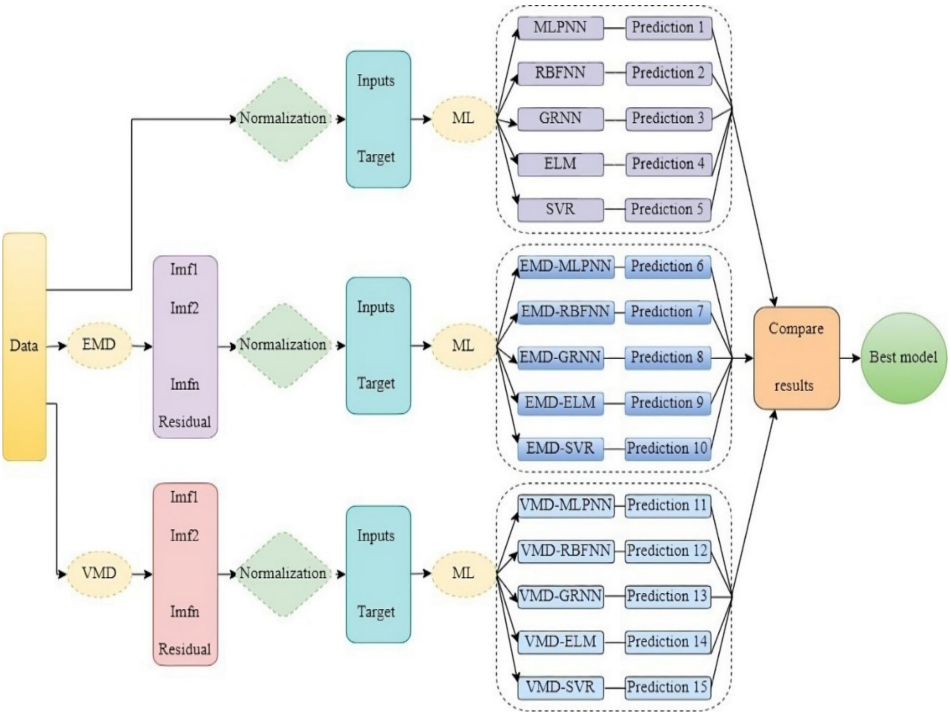

Figure 12: Schematic diagram of the proposed methodology model

Table 3: Performance results of simple and hybrid ML models

		Training		
Models	**R**	**NSE**	**RMSE (m^3/day)**	**MAE (m^3/day)**
MLPNN	0.8616	0.7405	13.5976	8.7801
RBFNN	**0.8803**	**0.7748**	**12.6668**	**8.5068**
GRNN	0.7965	0.5542	17.8233	12.6704
ELM	0.8398	0.7052	14.4942	10.1054
SVR	0.8417	0.7057	14.4817	10.5600
EMD-MLPNN	**0.9729**	**0.9448**	**6.2735**	**2.5521**
EMD-RBFNN	0.8331	0.6930	14.7896	10.9594
EMD-GRNN	0.9607	0.9203	7.5361	4.2452
EMD-ELM	0.8135	0.6617	15.5260	10.6347
EMD-SVR	0.8969	0.7955	12.0718	9.9499
VMD-MLPNN	0.8478	0.7177	14.1835	9.9872
VMD-RBFNN	0.7962	0.6334	16.1615	12.1602
VMD-GRNN	0.8995	0.7948	12.0922	7.9996
VMD-ELM	0.8160	0.6659	15.4298	11.0728
VMD-SVR	**0.9119**	**0.8297**	**11.0172**	**6.7368**

Testing				
Models	R	NSE	RMSE (m^3/day)	MAE (m^3/day)
MLPNN	0.9110	0.8258	12.6816	9.3145
RBFNN	**0.9109**	**0.8277**	**12.6108**	**9.5772**
GRNN	0.7391	0.3954	23.6234	17.4487
ELM	0.6671	0.4422	22.6905	17.0265
SVR	0.7267	0.5108	21.2498	15.9028
EMD-MLPNN	**0.9909**	**0.9815**	**4.1319**	**2.1144**
EMD-RBFNN	0.8761	0.7507	15.1704	11.4676
EMD-GRNN	0.9811	0.9608	6.0156	3.1790
EMD-ELM	0.3589	-0.1163	32.1002	26.9474
EMD-SVR	0.6371	-1.7157	50.0679	42.8947
VMD-MLPNN	0.8528	0.7272	15.8699	11.3517
VMD-RBFNN	0.8444	0.7046	16.5134	12.1541
VMD-GRNN	**0.9393**	**0.8394**	**12.1761**	**8.5774**
VMD-ELM	0.5974	0.3423	24.6401	18.8153
VMD-SVR	0.3501	-0.0629	31.3223	23.5982

Simple ML

The quantitative results of the simple ML models are presented in Table 3. For the training phase, the RBFNN model showed higher performance parameters (R = 0.88 and NSE = 0.77) and lower errors (RMSE = 12.67, MAE = 8.51), MLPNN (R = 0.86, NSE = 0.74, RMSE = 13.6, and MAE = 8.78) than SVR (R = 0.84, NSE = 0.71, RMSE = 14.48, and MAE = 10.56). In the testing phase, RBFNN model efficiency presented the highest performance parameters (R = 0.91 and NSE = 0.82) and lower errors (RMSE = 12.61, MAE = 9.58) compared to the MLPNN (R = 0.91, NSE = 0.82, RMSE = 12.68, and MAE = 9.31) and SVR models (R = 0.73, NSE = 0.51, RMSE = 21.25, and MAE = 15.9). The performance of ML models for the testing stage is exhibited in the time series graphs and the scatter plots in Fig. 13, which shows the efficiency of the RBFNN model. Such a model nearly predicted DS and had a higher performance parameter (R = 0.91) and a lower error (MAE = 9.31).

The Taylor diagram was used as a simple tool to display the details of the predictive models (Taylor, 2001). It is the most general suggested diagram for comparing accuracy because of the benefits of combining and measuring many statistical performance indicators and was used as a simple tool to visualize the details of the predictive models in this study. When the predicted values are close to the observed values, this indicates that they are predictive in terms of standard deviation (SD), their correlation (R) is high and close to 1, and their root mean square deviation (RMSD) is low and close to 0. The correlation decreases if a value goes to higher zones in the diagram. RMSD indicates the quality of the simulation procedure. Based on Fig. 14a, the RBFNN model's SD predicted = 25.36 is more than the SD of the other ML models and is less than the SD observed = 28.34, which shows that underestimation occurs. The higher correlation R = 0.89 shows a high level of agreement between the observed and predicted values, and the RMSD is the least and close to 12 in comparison with the other ML models.

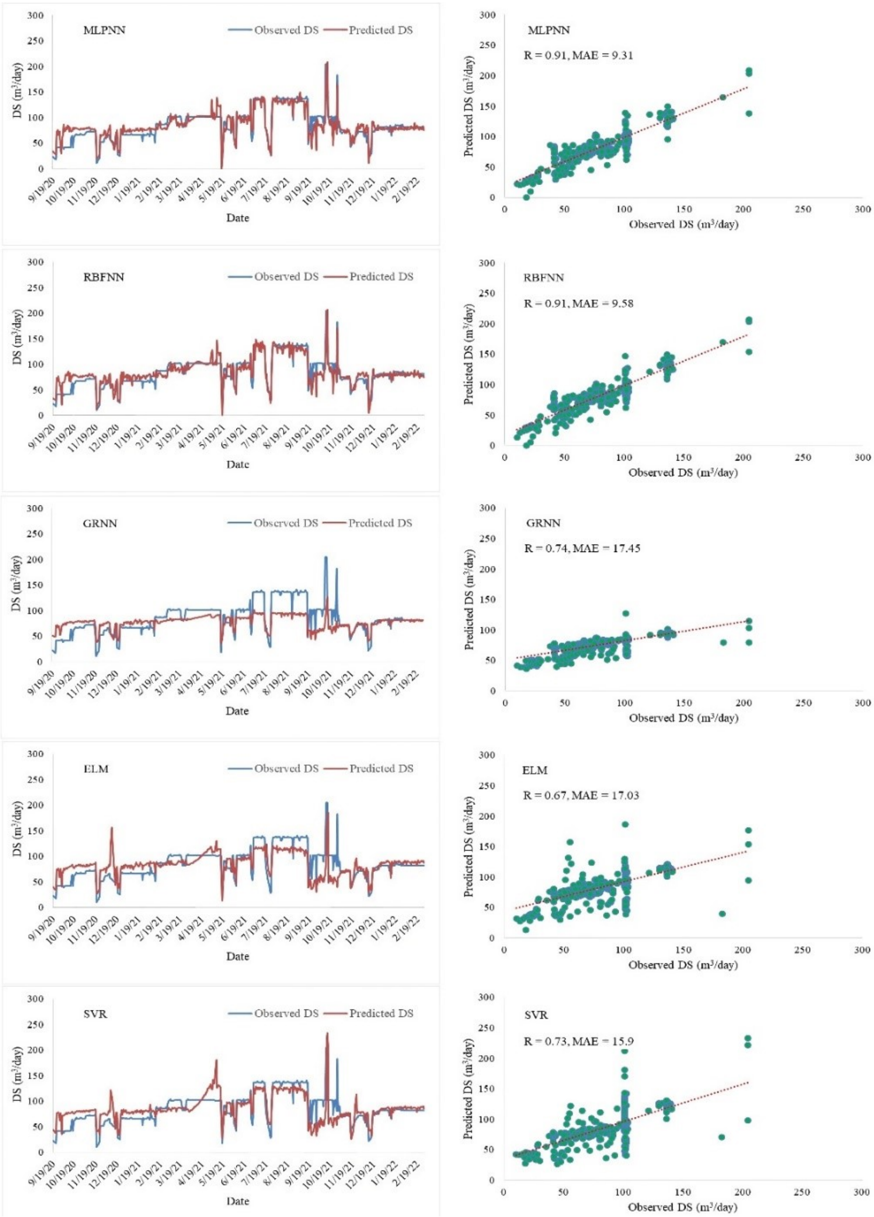

Figure 13: Time series graphs and scatter plots using ML models for the testing phase

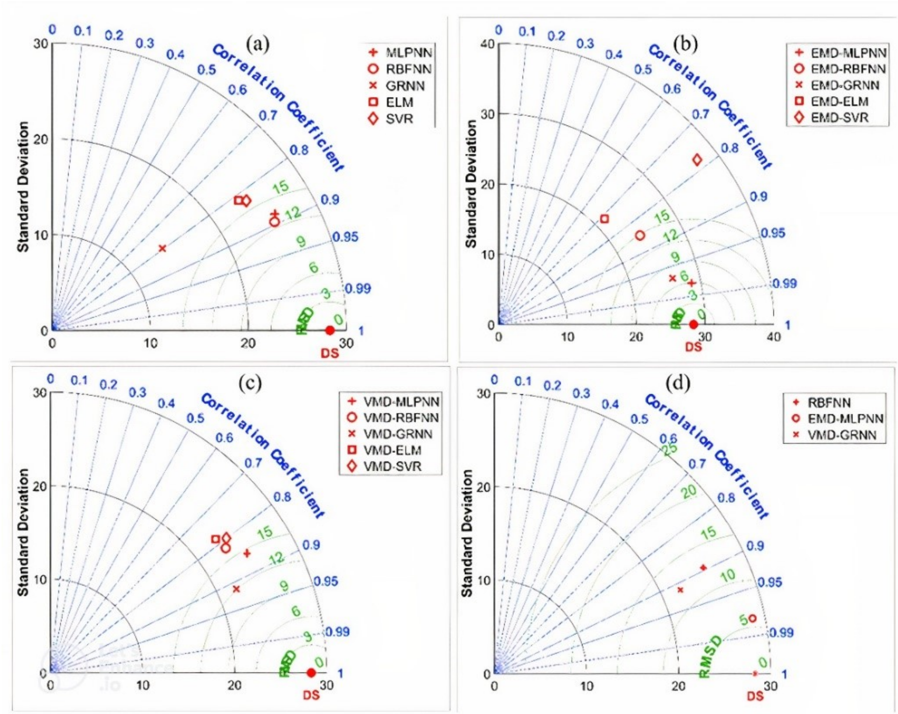

Figure 14: Taylor diagram presentation for different: (a) ML, (b) EMD-ML, (c) VMD-ML, (d) best predictive models

Hybrid EMD-ML

The results of the hybrid EMD-ML models are presented in Table 3. The latter indicates that the EMD-MLPNN model had lower errors (RMSE = 6.27, MAE = 2.55) and EMD-GRNN (RMSE = 7.54, MAE = 4.25) than EMD-SVR (RMSE = 12.07, MAE = 9.95) in the training phase. The study of hybrid EMD-ML model efficiency indicated that the EMD-MLPNN model showed the highest performance parameters (R = 0.99, NSE = 0.98) and EMD-GRNN (R = 0.98, NSE = 0.96) compared to EMD-RBFNN (R = 0.88, NSE = 0.75) in the testing phase.

The performance of the EMD-ML models is exhibited in Fig. 15, which proves EMD-MLPNN's efficiency. This model closely predicts DS, with the lowest error (MAE = 2.11) and a higher performance parameter (R = 0.99), but the remaining models are inadequate compared to it.

Fig. 14b shows that the EMD-MLPNN model had a high correlation of 0.97 that was close to 1, SD = 28.65 and was more than the SD observed values, which signifies that the EMD-MLPNN model overestimates the DDSP, and the RMSD is the least and close to 6 in comparison with the other EMD-ML models.

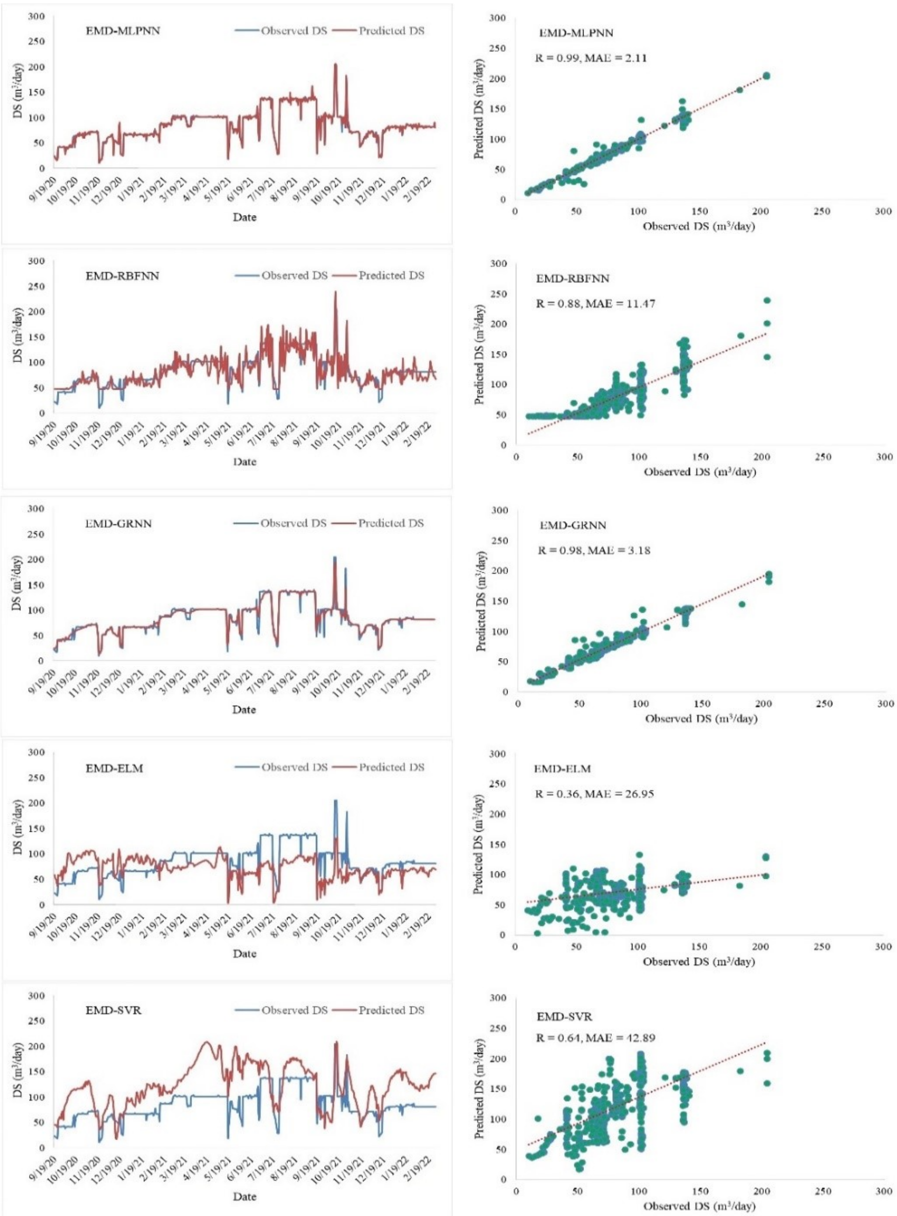

Figure 15: Time series graphs and scatter plots using EMD-ML models for the testing phase

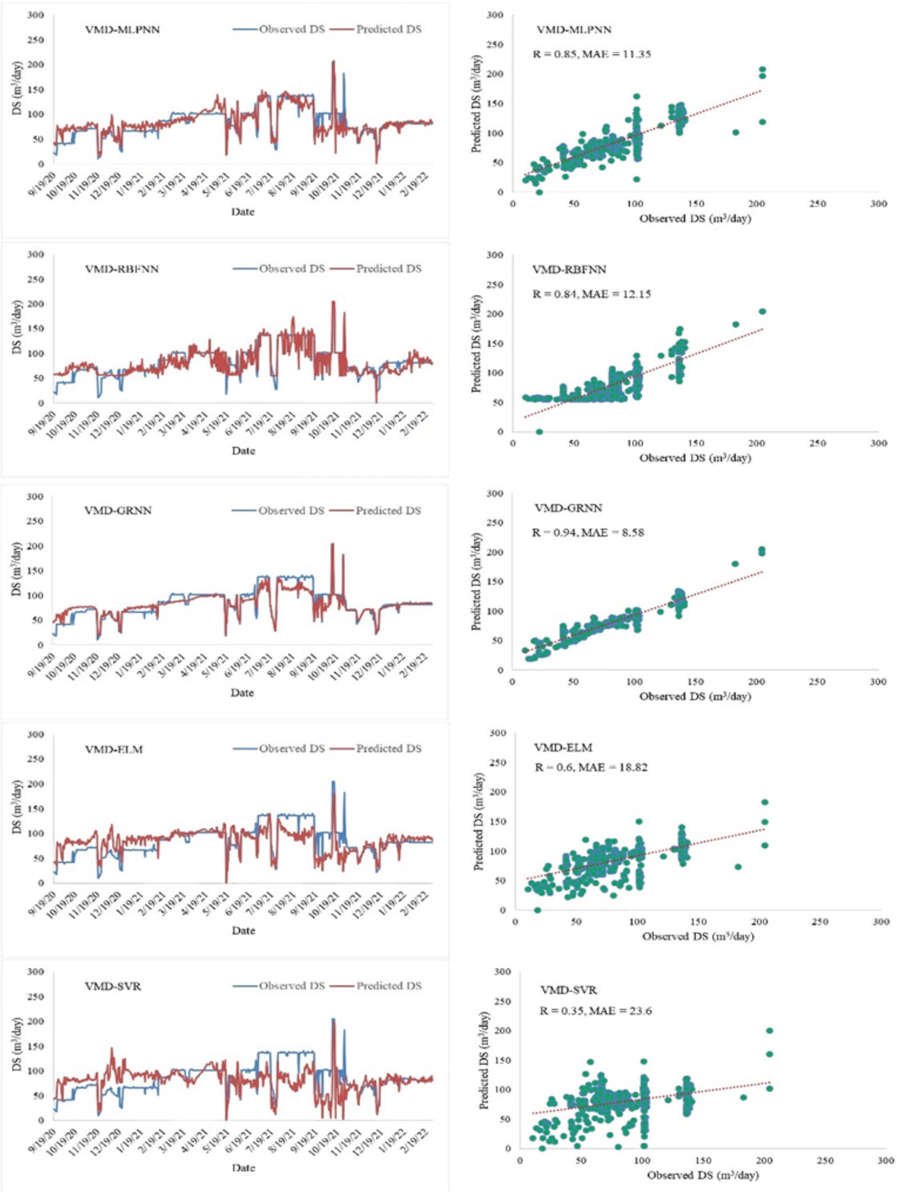

Figure 16: Time series graphs and scatter plots using VMD-ML models for the testing phase

Hybrid VMD-ML

The performance of the hybrid VMD-ML models is presented in Table 3. With regard to the training stage, the VMD-SVR model shows an efficiency higher performance parameters level (R = 0.91, NSE = 0.83) and lower errors (RMSE = 11.02, MAE = 6.74), regarding VMD-GRNN (R = 0.9, NSE = 0.79, RMSE = 12.09, and MAE = 8), than VMD-MLPNN (R = 0.85, NSE = 0.72, RMSE = 14.18, and MAE = 9.99). For the testing stage, the study of hybrid VMD-ML model efficiency designated that the performance of the VMD-GRNN model presents the highest performance parameters (R = 0.94, NSE = 0.84) and lower errors (RMSE = 12.18, MAE = 8.58), VMD-MLPNN (R = 0.85, NSE = 0.73, RMSE = 15.87, and MAE = 11.35) than VMD-RBFNN (R = 0.84, NSE = 0.7, RMSE = 16.51, and MAE = 12.15).

Fig. 16 shows the performance of VMD-ML models, which shows VMD-GRNN model efficiency with a relatively higher performance (R = 0.93) and a lower error (MAE = 8.57).

The Taylor diagram in Fig. 14c shows that the VMD-GRNN model's SD predicted = 22.13 is more than those of the VMD-ML models and less than the SD observed. This indicates that underestimation occurs. A higher correlation of 0. 91 points to a higher level of agreement between observed and predicted values, and the RMSD is the least and close to 12 in comparison with the other VMD-ML models.

Best of proposed models

The qualitative results are presented in Table 4. After comparing the statistical parameters for predicting the daily dried sludge production, it was observed that the EMD-MLPNN outperformed the two other models, VMD-GRNN and RBFNN, which led to the highest degree of accuracy in performance parameters and to the lowest errors.

Table 4: Performance results of the best models

			Training	
Models	**R**	**NSE**	**RMSE (m^3/day)**	**MAE (m^3/day)**
RBFNN	0.8803	0.7748	12.6668	8.5068
EMD-MLPNN	**0.9729**	**0.9448**	**6.2735**	**2.5521**
VMD-GRNN	0.8995	0.7948	12.0922	7.9996

			Testing	
Models	R	NSE	RMSE (m^3/day)	MAE (m^3/day)
RBFNN	0.9109	0.8277	12.6108	9.5772
EMD-MLPNN	**0.9909**	**0.9815**	**4.1319**	**2.1144**
VMD-GRNN	0.9393	0.8394	12.1761	8.5774

Relying on the graphical interpretation (Figure 14d), the EMD-MLPNN had the highest value of correlation R = 0.97 and SD = 28.65 of the predicted values were less than the R and SD of VMD-GRNN and RBFNN. This shows the hybrid model EMD-MLPNN capacity in the nonlinear procedure, as MLPNN proved great performance when modeling and predicting within the scope of environmental engineering.

In comparison to previous investigations, Najafzadeh and Zeinolabedini (2018) found that the W-MT model had performance parameters that reached R = 0.99, NSE = 0.98 and errors reaching MAE = 6.29 and RMSE = 8.15. Zeinolabedini and Najafzadeh (2019) indicated that the statistical values of the W-FFBPNN model were MAE = 5.79, RMSE = 7.76, and R= 0.98. Djeddou et al. (2021) specified the PCA-FFBPNN model with the following performance parameters: R = 0.99, RMSE = 5.56, MAE = 3.99, and NSE = 0.98. Relying on such a comparison, it can be confirmed that the current study has reached roughly similar parameters regarding R and NSE, but lesser error values (RMSE and MAE) were found. It can thus be confirmed that the suggested EMD-MLPNN prediction model in this work has the highest level of accuracy and can be used to predict sludge quantity in WWTPs.

The research findings indicate that out of all the models considered, the EMD-MLPNN model is the most appropriate. EMD, a preprocessing technique for signals, partitions the signal into a series of IMFs. These IMFs are often used to describe the different oscillatory modes within a signal and are typically characterized by three properties: zero mean, finite energy, and symmetrical extrema.

Using EMD with ANNs in prediction has several advantages. More accurate predictions can be made by focusing on the underlying oscillatory modes of the signal, rather than being influenced by the overall trend or noise present in the signal, especially when the oscillatory modes are more relevant to the prediction task than the trend or noise. Furthermore, decomposing the signal into IMFs using this method provides a more intuitive and comprehensible representation of the signal for the ANN.

In contrast, the VMD approach does not employ a filtering process in its decomposition operation, which gives it an advantage in dealing with mode mixing issues. This approach ensures a more accurate decomposition result because it uses a combination of Wiener filtering, Hilbert transform, and the alternate direction method of the multiplier to properly breakdown any signal into sets of variational mode functions (VMFs) without discarding any crucial information from the original signal.

CONCLUSION

In this study, various ML models combined with different decomposition techniques, specifically EMD and VMD, were employed to predict DDSP in the Aïn Beïda WWTP, Algeria. A comparative analysis was conducted between simple ML models and hybrid ML models to identify the most accurate predictive model.

The results obtained from the simple ML models demonstrated that the RBFNN method exhibited the best statistical performance during the training phase (R = 0.8803, RMSE = 12.6668 m^3/day). In the testing phase, R and MSE equalled 0.9109 and 12.6108 m^3/day, respectively, outperforming the other ML models.

Among the hybrid EMD-ML models, the EMD-MLPNN method yielded the most accurate prediction results. During the training phase, R reached 0.9729, and RMSE reached 6.2735 m^3/day. In the testing phase, R = 0.9909 and RMSE= 4.1319 m^3/day, surpassing the other EMD-ML models.

Comparing the VMD-ML models, the hybrid VMD-GRNN method exhibited the best performance during the training phase with R = 0.8995 and RMSE = 12.0922 m^3/day. In the testing phase, it achieved an R = 0.9393 and an RMSE = 12.1761 m^3/day.

The findings indicated that the EMD-MLPNN model outperformed the VMD-GRNN and RBFNN models. In the training phase, it achieved a good performance with R that equalled 0.9729, NSE = 0.9448, and RMSE = 6.2735 m^3/day. In the testing phase, it reached 0.9909 for R, 0.9815 for NSE, and RMSE reached 4.1319 m^3/day. These results highlight the high generalization capacity of the proposed model, EMD-MLPNN, which can be attributed to the hybridization of inputs using EMD.

Declaration of competing interest

The authors declare that they have no known competing financial interests or personal relationships that could have appeared to influence the work reported in this paper.

ACKNOWLEDGEMENTS

We would like to thank the manager of the Aïn Beïda wastewater treatment plant for providing us with the field data used in this study.

REFERENCES

ABDA Z., CHETTIH M. (2018). Forecasting daily flow rate based intelligent hybrid models combining wavelet and Hilbert-Huang transforms in the Mediterranean basin in northern Algeria, Acta Geophysica, Vol. 66, Issue 5, pp. 1131–1150.

ABDA Z., CHETTIH M., ZEROUALI B. (2021). Assessment of neuro-fuzzy approach based different wavelet families for daily flow rates forecasting, Modeling Earth Systems and Environment, Vol. 7, pp. 1523–1538.

AHMED A.A.M., JUI S.J.J., CHOWDHURY M.A.I., AHMED O., SUTRADHA A. (2022). The development of dissolved oxygen forecast model using hybrid machine learning algorithm with hydrometeorological variables, Environmental Science and Pollution Research, Vol. 30, Issue 3, pp. 7851-7873.

AROUA-BERKAT S., AROUA N. (2022). Opportunities and challenges for wastewater reuse in Algeria, Larhyss Journal, No 51, pp. 7-17.

BAGHERI M., MIRBAGHERI S.A., BAGHERI Z., KAMARKHANI A.M. (2015). Modeling and optimization of activated sludge bulking for a real wastewater treatment plant using hybrid artificial neural networks-genetic algorithm approach, Process Safety and Environmental Protection, Vol. 95, pp. 12-25.

BAKI O.T., ARAS E. (2018). Estimation of BOD in wastewater treatment plant by using different ANN algorithms, Membrane Water Treatment, Vol. 9, Issue 6, pp. 455-462.

BAKI O.T., ARAS E., AKDEMIR U.O., YILMAZ B. (2019). Biochemical oxygen demand prediction in wastewater treatment plant by using different regression analysis models, Desalination and Water Treatment, Vol. 157, pp. 79–89.

BELANCHE L.A., VALDES J.J., COMAS J., RODA I.R., POCH M. (1999). Towards a model of input–output behaviour of wastewater treatment plants using soft computing techniques, Environmental Modelling and Software, Vol. 14, Issue 5, pp. 409-419.

BONIECKI P., DACH J., PILARSKI K., PIEKARSKA-BONIECKA H. (2012). Artificial neural networks for modeling ammonia emissions released from sewage sludge composting, Atmospheric Environment, Vol. 57, pp. 49-54.

CAI Q.C., HSU T.H., LIN J.Y. (2021). Using the General Regression Neural Network Method to Calibrate the Parameters of a Sub-Catchment, Water, Vol. 13, Issue 8, pp.1-12.

CONG Q., YU W. (2018). Integrated soft sensor with wavelet neural network and adaptive weighted fusion for water quality estimation in wastewater treatment process, Measurement, Vol. 124, Issue 27-33, pp. 436-446.

DJEDDOU M., ACHOUR B. (2015). The use of a neural network technique for the prediction of sludge volume index in municipal wastewater treatment plant, Larhyss Journal, No 24, pp. 351-370.

DJEDDOU M., HAMEED I.A., NEJATIAN A., LOUKAM I. (2020). Predictive Modelling of COVID-19 New Cases in Algeria using An Extreme Learning Machines (ELM), MedRxiv preprint, 18 pages.

DJEDDOU M., HELLAL A., LOUKAM I., HAMEED I.A. (2021a). Application of Hybrid Principal Component Analysis-Artificial Neural Network to Predict Daily Digested Sludge production in Full-scale Wastewater Treatment Plant, In 5th International Water Association (IWA) Specialized International Conference Eco-technologies for Wastewater Treatment (ecoSTP), Milan, Italy, 6 pages.

DJEDDOU M., HELLAL A., LOUKAM I., HOUICHI L. (2021b). Predictive modeling of ozone dosing in Full-scale drinking water treatment plant using Improved Hybrid Model Based on Discrete Wavelet Decomposition and Radial Basis Function Neural Network (WRBFNN), In 3rd International Water Association (IWA) Specialized International Conference on Disinfection and DBPs, Milan, Italy, pp. 57-60.

DJEDDOU M., ZHAO X., HAMEED I.A., RAHMANI A. (2021c). Hybrid Improved Empirical Mode Decomposition and Artificial Neural Network Model for the Prediction of Critical Heat Flux (CHF), In 28th International Conference on Nuclear Engineering (ICONE 28), American Society of Mechanical Engineers, USA, Vol. 2, 9 Pages.

DRAGOMIRETSKIY K., ZOSSO D. (2013). Variational mode decomposition. IEEE Transactions on Signal Processing, Vol. 62, Issue 3, pp. 531-544.

EL GHAMMAT A., TEMSAMANI RIFFI K., HASSANI ZERROUK M. (2019). A study of the performance of a sequential bioreactor plant for the treatment of dairy effluents, Larhyss Journal, No 37, pp. 7-21. (In French)

FOUCHAL A, SOUAG-GAMANE D. (2019). Long-term monthly stream-flow forecasting in humid and semiarid regions, Acta Geophysica, Vol. 67, pp. 1223–1240.

GAOUAR Y.M., GAOUAR B.N. (2016). Best available technology assessment of three existing processes in waste water treatment field, Larhyss Journal, No 27, pp. 105-123. (In French)

GONTARSKI C.A., RODRIGUES P.R., MORI M., PRENEM L.F. (2000). Simulation of an industrial wastewater treatment plant using artificial neural networks, Computers and Chemical Engineering, Vol. 24, Issues 2-7, pp. 1719-1723.

GOOGLE (2023). Aïn Beïda wastewater treatment plant cardiff, Available at: https://earth.google.com/web/@35.7882968,7.33849481,928.45273645a,575.97066821d,35y,0 h,00r, Accessed 24 February 2023.

GUO H., JEONG K., LIM J., JO, J., KIM, Y. M., PARK, J. P., KIM, J. H., CHO, K. H. (2015). Prediction of effluent concentration in a wastewater treatment plant using machine learning models, Journal of Environmental Sciences, Vol. 32, pp. 90-101.

HANBAY D., TURKOGLU I., DEMIR Y. (2008). Prediction of wastewater treatment plant performance based on wavelet packet decomposition and neural networks, Expert Systems with Applications, Vol. 34, Issue 2, pp. 1038-1043.

HAYKIN S. (2009). Neural networks and learning machines, Third edition, Pearson Education, India.

HBAIZ E.M., SATIF C., FATH-ALLAH R., LEBKIRI M., LEBKIRI A., RIFI E.H. (2014). Effect of sludge of wastewater from the treatment plant on the growth in pepper (*Capsicum Annuum.l*) cultivated on two different grounds, Larhyss Journal, No 20, pp. 43-55.

HEDDAM S., KISI O. (2017). Extreme learning machines: a new approach for modeling dissolved oxygen (DO) concentration with and without water quality variables as predictors, Environmental Science and Pollution Research, Vol. 24, Issue 20, pp. 16702–16724.

HONG H., ZHANG Z., GUO A., SHEN L., SUN H., LIANG Y., WU F., LIN H. (2020). Radial basis function artificial neural network (RBF ANN) as well as the hybrid method of RBF ANN and grey relational analysis able to well predict trihalomethanes levels in tap water, Journal of Hydrology, Vol. 591, pp.1-11.

HUANG G.B. (2003). Learning capability and storage capacity of two hidden layer feed-forward networks, IEEE Transactions on Neural Networks, Vol. 14, Issue 2, pp. 274-281.

HUANG G.B., ZHU Q.Y., SIEW C.K. (2006). Extreme learning machine: theory and applications, Neurocomputing, Vol. 70, Issue 1-3, pp. 489-501.

HUANG N.E., SHEN Z., LONG S.R., WU M.C., SHIH H.H., ZHENG Q., YEN N.C., TUNG C.C., LIU H.H. (1998). The empirical mode decomposition and the Hilbert spectrum for nonlinear and non-stationary time series analysis, Proceedings of the Royal Society A: Mathematical, Physical and Engineering Sciences, Vol. 454, Issue 1971, pp. 903-998.

HUANG Y.W., CHEN M.Q. (2015). Artificial neural network modeling of thin layer drying behavior of municipal sewage sludge, Measurement, Vol. 73, pp. 640-648.

KHATRI N., KHATRI K.K., SHARMA A. (2019). Prediction of effluent quality in ICEAS-sequential batch reactor using feed-forward artificial neural network, Water Science and Technology, Vol. 80, Issue 2, pp. 213–222.

LEONG W.C., BAHADORI A., ZHANG J., AHMAD Z. (2019). Prediction of water quality index (WQI) using support vector machine (SVM) and least square-support vector machine (LS-SVM), International Journal of River Basin Management, Vol. 19, Issue 2, pp. 149-156.

LI F.F., WANG Z.Y., QIU J. (2019). Long-term stream-flow forecasting using artificial neural network based on preprocessing technique, Journal of Forecasting, Vol. 38, Issue 3, pp.192-206.

MANSOUR-BAHMANI A., HAGHIABI A.H., SHAMSI Z., PARSAIE A. (2021). Predictive modeling the discharge of urban wastewater using artificial intelligent models (case study: Kerman city), Modeling Earth Systems and Environment, Vol. 7, Issue 3, pp. 1917- 1925.

MJALLI F.S., AL-ASHEH S., ALFADALA H.E. (2007). Use of artificial neural network black-box modeling for the prediction of wastewater treatment plants performance, Journal of Environmental Management, Vol. 83, Issue 3, pp. 329-338.

MOODY J., DARKEN C.J. (1989). Fast learning in networks of locally tuned processing units, Neural Computation, Vol. 1, Issue 2, pp. 281-294.

NAJAFZADEH M., ZEINOLABEDINI M. (2018). Derivation of optimal equations for prediction of sewage sludge quantity using wavelet conjunction models: an environmental assessment, Environmental Science and Pollution Research, Vol. 25, Issue 23, pp. 22931-22943.

NAJAFZADEH M., ZEINOLABEDINI M. (2019). Prognostication of waste water treatment plant performance using efficient soft computing models: An environmental evaluation, Measurement, Vol. 138, pp. 690–701.

NASR M.S., MOUSTAFA M.A.E., SEIF H.A.E., KOBROSY G.E. (2012). Application of Artificial Neural Network (ANN) for the prediction of EL-AGAMY wastewater treatment plant performance-EGYPT, Alexandria Engineering Journal, Vol. 51, Issue 1, pp. 37-43.

ONKAL-ENGIN G., DEMIR I., ENGIN S.N. (2005). Determination of the relationship between sewage odour and BOD by neural networks, Environmental Modelling and Software, Vol. 20, Issue 7, pp. 843-850.

PAI T.Y., YANG P.Y., WANG S.C., LO M.H., CHIANG C.F., KUO J.L., CHU H.H., SU H.C., YU L.F., HU H.C., CHANG Y.H. (2011). Predicting effluent from the wastewater treatment plant of industrial park based on fuzzy network and influent quality, Applied Mathematical Modelling, Vol. 35, Issue 8, pp. 3674-3684.

RAYI V.K., MISHRA S.P., NAIK J., DASH P.K. (2022). Adaptive VMD based optimized deep learning mixed kernel ELM auto-encoder for single and multistep wind power forecasting, Energy, Vol. 244, pp.1-29.

SONG C., YAO L., HUA C., NI Q. (2021). A water quality prediction model based on variational mode decomposition and the least squares support vector machine optimized by the sparrow search algorithm (VMD-SSA-LSSVM) of the Yangtze River, China, Environmental Monitoring and Assessment, Vol. 193, Issue 6, pp. 1-17.

SPECHT D.F. (1991). A general regression neural network, IEEE Transactions on Neural Networks, Vol. 2, Issue 6, pp. 568-576.

TAYLOR K.E. (2001). Summarizing multiple aspects of model performance in a single diagram, Journal of Geophysical Research, Vol. 106, Issue D7, pp. 7183-7192.

VAPNIK V. (1999). The nature of statistical learning theory, Springer science and business media, Second Edition, USA.

VERMA A., WEI X., KUSIAK A. (2013). Predicting the total suspended solids in wastewater: a data-mining approach, Engineering Applications of Artificial Intelligence, Vol. 26, Issue 4, pp. 1366-1372.

WANG Z., SHAO D., YANG H., YANG S. (2015). Prediction of water quality in South to North Water Transfer Project of China based on GA-optimized general regression neural network, Water Science and Technology: Water Supply, Vol. 15, Issue 1, pp.150-157.

WONGBURI P., PARK J.K. (2022). Prediction of Sludge Volume Index in a Wastewater Treatment Plant Using Recurrent Neural Network, Sustainability, Vol. 14, Issue 10, pp. 62-76.

YANG Y., WANG P., GAO X. (2022). A novel radial basis function neural network with high generalization performance for nonlinear process modelling, Processes, Vol. 10, Issue 1, pp.1-16.

YILMAZ M., TOSUNOĞLU F., KAPLAN N.H., ÜNEŞ F., HANAY Y.S. (2022). Predicting monthly streamflow using artificial neural networks and wavelet neural networks models, Modeling Earth Systems and Environment, Vol. 8, Issue 4, pp. 5547-5563.

ZAKHROUF M., BOUCHELKIA H., STAMBOUL M., KIM S, SINGH V.P. (2020). Implementation on the evolutionary machine learning approaches for streamflow forecasting: Case study in the Seybous River, Algeria, Journal of Korea Water Resources Association, Vol. 53, Issue 6, pp. 395-408.

ZARE ABYANEH H. (2014). Evaluation of multivariate linear regression and artificial neural networks in prediction of water quality parameters, Journal of Environmental Health Science & Engineering, Vol. 12, Issue 1, pp. 1-8.

ZEINOLABEDINI M., NAJAFZADEH M. (2019). Comparative study of different wavelet-based neural network models to predict sewage sludge quantity in wastewater treatment plant, Environmental Monitoring and Assessment, Vol. 191, Issue 3, pp. 1-25.

ZEROUALI B., SANTOS C.A.G., DE FARIAS C.A.S., MUNIZ R.S., DIFI S., ABDA Z., CHETTIH M., HEDDAM S., ANWAR S.A., ELBELTAGI A., (2023). Artificial intelligent systems optimized by metaheuristic algorithms and teleconnection indices for rainfall modeling: The case of a humid region in the mediterranean basin, Heliyon, Vol. 9, Issue 4, pp. 1-17.